^{18}F-FDG PET/CT can differentiate vertebral metastases from Schmorl's nodes by distribution characteristics of the ^{18}F-FDG

Zhengming Wang[1] MD,
Leilei Yuan[1] MD,
***Daqing Ma[2] MD, PhD,**
***Jigang Yang[1] MD, PhD**

**Jigang Yang, Daqing Ma contributed equally to this work and should be considered as co-corresponding authors*

1. Department of Nuclear Medicine, Beijing Friendship Hospital, Capital Medical University, 95 Yong An Road, Xi Cheng district, Beijing, 100050, People's Republic of China
2.Department of Radiology, Beijing Friendship Hospital, Capital Medical University, 95 Yong An Road, Xi Cheng district, Beijing, 100050, People's Republic of China

Keywords: - ^{18}F-FDG PET/CT
- Schmorl's nodes
- Vertebral metastases

Corresponding author:
Jigang Yang,
Department of Nuclear Medicine, Beijing Friendship Hospital, Capital Medical University, 95 Yong An Road, Xi Cheng district, Beijing, 100050, People's Republic of China
13681221974@163.com
13121275863@163.com

Received:
12 August 2016
Accepted revised:
5 October 2016

Abstract

Background: Differentiation of vertebral metastases from Schmorl's nodes, especially with fluorine-18-fluorodeoxyglucose (^{18}F-FDG) uptake, is very important for the appropriate management of these patients in case they have malignancy. We aimed to evaluate the value of ^{18}F-FDG positron emission tomography/computed tomography (PET/CT) in differentiating vertebral metastases from Schmorl's nodes with ^{18}F-FDG uptake. **Subjects and Methods:** Fourteen patients with malignancy underwent ^{18}F-FDG PET/CT, which showed abnormal ^{18}F-FDG uptake in 19 Schmorl's nodes. Twenty one patients with vertebral metastases underwent ^{18}F-FDG PET/CT, which showed abnormal ^{18}F-FDG uptake in 28 vertebral metastatic lesions. All these Schmorl's nodes and vertebral metastases were confirmed by pathology or by follow-up. The ^{18}F-FDG PET/CT were retrospectively analyzed, including maximum standardized uptake value (SUVmax), the distribution characteristic of ^{18}F-FDG and the size of these lesions in PET and CT. **Results:** The mean value of SUVmax of Schmorl's nodes with ^{18}F-FDG uptake were 5.7±2.8, while the mean value of SUVmax of vertebral metastases were 6.6±3.2. There were no significant differences in the SUVmax between Schmorl's nodes and vertebral metastases. However, the ^{18}F-FDG distribution in Schmorl's nodes and vertebral metastases showed some differences. The ^{18}F-FDG uptake in the bordeline area surrounding the nucleus pulposus was highter in Schmorl's nodes. The size of Schmorl's nodes on PET was significantly smaller than that on CT. The size of vertebral metastases on PET was larger or similar with that on CT. **Conclusion:** Although the SUVmax in the Schmorl's nodes and vertebral metastases was similar, the ^{18}F-FDG distribution characteristic in PET/CT can help differentiating the vertebral metastases from Schmorl's nodes.

Hell J Nucl Med 2016; 19(3): 241-244 *Epub ahead of print: 8 November 2016* *Published online: 10 December 2016*

Introduction

Schmorl's nodes were considered as a herniation of the nucleus pulposus through the cartilaginous and bony endplate into the vertebral body [1]. Schmorl's nodes present most commonly as incidental findings in asymptomatic patients or in patients with back or radicular pain due to different etiologies [1]. It is essential for appropriate management to differentiate Schmorl's nodes from vertebral metastases in case Schmorl's nodes were demonstrated incidentally in patients with a history of malignancy. Spine is a common bone metastases site in patients with malignancy. However, the differential diagnosis of Schmorl's nodes from vertebral metastases is still challenging in clinical practice.

Fluorine-18-fluorodeoxyglucose positron emission tomography/computed tomography (^{18}F-FDG PET/CT) has been used in diagnosing and staging benign diseases [2], such as Schmorl's node [3], and malignant diseases [4, 5], such as bone metastases [6]. Lin et al. (2012) reported that Schmorl's nodes had low to moderate ^{18}F-FDG PET/ CT uptake, which could cause false positive results in patient with malignancy [3]. The aim of this study was to study the ^{18}F-FDG PET/CT image and especially the ^{18}F-FDG PET/CT distribution characteristics in differentiating vertebral metastases from Schmorl's nodes.

Case Report

Between January 2009 and December 2014, 14 patients with a history of malignancy, 8 male and 6 female; mean age 58.7±10.8 years old were diagnosed with Schmorl's nodes

(Schmorl's node group). The malignancies of this group included 4 patients with lung cancer, 3 with breast cancer, 3 with digestive system cancer, 2 with prostate cancer, 1 with liver cancer and 1 with ovarian cancer. During the same period, 21 patients also with a history of malignancy (11 male and 10 female, mean age 60.2±9.6 years) were diagnosed with vertebral metastases (vertebral metastases group). The malignancies of the vertebral metastases group included 7 patients with lung cancer, 4 with digestive system cancer, 3 with liver cancer, 3 with breast cancer, 2 with prostate cancer, 1 with ovarian cancer and 1 with nasopharyngeal cancer. The diagnosis of Schmorl's nodes and vertebral metastases was based on pathology and/or follow- up. The follow-up time was between 6-42 months, mean 16.8±9.6 months. A physician could not differentiate vertebral metastases from Schmorl's nodes before the ^{18}F-FDG PET/CT scan. All these patients underwent the ^{18}F-FDG PET/CT scan. The ^{18}F-FDG PET/CT of Schmor's node group showed ^{18}F-FDG uptake in the Schmor's node. The ^{18}F-FDG PET/CT images were studied retrospectively, including qualitative and semi-quantitative analysis. This study was approved by the Beijing Friendship Hospital, Capital Medical Universtiy ethics committee.

^{18}F-FDG PET/CT imaging protocol and data analysis

Each patient was asked to fast for at least 6 hours before ^{18}F-FDG PET/CT imaging. All scans were performed on a combined PET/CT scanner (Discovery LS; GE Healthcare, Milwaukee, WI). Fluorine-18-FDG PET/CT images of each patient were acquired approximately 60min after the intravenous injection of ^{18}F-FDG. In addition, their serum blood glucose levels were measured before the injection of ^{18}F-FDG, and if the level of glucose was over 6.7mmol/L, the examination was deferred.

An unenhanced CT scan was performed first for PET attenuation correction and then PET data were acquired in two dimensional (2D) mode, for 3.5min of acquisition time per bed position. The CT images were reconstructed onto a 512× 512 matrix with a section thickness of 3.75mm. Using the CT data for attenuation correction, the images were then reconstructed with an ordered set expectation maximization (OSEM) algorithm. At the conclusion of the ^{18}F-FDG PET/CT scan, all reconstructed image data were transferred to a workstation for clinical evaluation and also to a local server for lesion volume data analysis. The SUVmax of Schmorl's nodules and vertebral metastases on ^{18}F-FDG PET/CT images were recorded.

Imaging analysis and measurement of ^{18}F-FDG PET/CT parameters

The ^{18}F-FDG PET/CT images were assessed by two experienced nuclear medicine physicians. Any discrepancy was resolved by consensus. The SUVmax, distribution characteristics of Schmorl's nodules and vertebral metastases of ^{18}F-FDG PET/CT were compared and analyzed.

Statistical analysis

The average value of SUVmax on ^{18}F-FDG PET/CT was expressed as mean±standard deviation (M±SD). The mean value of SUVmax of Schmorl's nodes and vertebral metastases on the ^{18}F-FDG PET/CT scan were compared using Wilcoxon's rank-sum test. The distribution characteristics of Schmorl's nodes and of vertebral metastases on the ^{18}F-FDG PET/CT scan were compared. All statistical tests were performed by using SPSS 20.0 software (SPSS. Inc., Chicago, IL, USA).

Results

Patients characteristics

In the Schmorl's nodes group, ^{18}F-FDG PET/CT showed ^{18}F-FDG uptake in 19 nodes of which 14 patients with malignancy. Eight of the 19 Schmorl's nodes were located in the thoracic vertebrae and 11 in the lumbar vertebrae. Five of these patients had two Schmorl's nodes and 9, a single Schmorl's node. The mean value of SUVmax of Schmorl's nodes with ^{18}F-FDG uptake was 5.7±2.8.

In vertebral metastases group, ^{18}F-FDG PET/CT showed ^{18}F-FDG uptake in 28 vertebral metastases of 21 patients with malignancy. Seven patients had two vertebral metastases and 14 a single vertebral metastasis. The mean value of SUVmax of vertebral metastases were 6.6±3.2. There was no significant difference in the SUVmax between Schmorl's nodes and vertebral metastases.

However, the ^{18}F-FDG distribution characteristics in Schmorl's nodes and vertebral metastases showed some differences. The ^{18}F-FDG uptake in the bordeline area surrounding the nucleus pulposus was higher than that of areas surrounding Schmorl's node. The size of Schmorl's nodes on the PET scan was significantly smaller than that on CT. Moreover, the higher ^{18}F-FDG uptake of these borderline areas surrounding the Schmorl's nodes were located around the nucleus pulposus (Figure 1). The size of vertebral metastases on the PET scan was larger or similar with that on CT (Figure 2).

Discussion

The differential diagnosis of Schmorl's nodes from vertebral metastases is essential in patients with malignancy. Different diagnostic methods have been used in the differential diagnosis, including CT [7], MRI [8] or ^{18}F-FDG PET/CT [3]. However, the differential diagnosis of the two diseases is still challenging in patients with malignancy. Previous studies have reported that Schmorl's nodes caused a false positive result on the ^{18}F-FDG PET/CT scan [3, 9].

Based on the present study, the mean value of SUVmax of Schmorl's nodes was similar with that of the vertebral metastases group. However, the ^{18}F-FDG distribution characteristics in Schmorl's nodes and vertebral metastases showed some differences.

Schmorl's node is herniation of nucleus pulposus through the cartilaginous and bony end plate into the body of an ad-

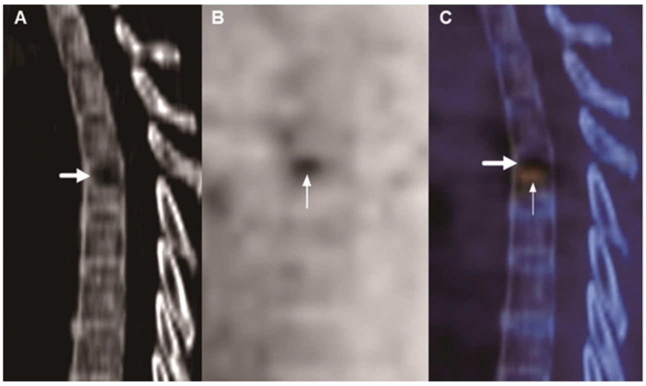

Figure 1. A 50 years old man with the history of lung cancer was diagnosed with Schmorl's nodes based on the ^{18}F-FDG PET/CT. The SUVmax of the Schmorl's nodes was 4.3. The size of Schmorl's nodes on PET (thin arrow in B) was smaller than that on CT (thick arrow in A). Moreover, the high ^{18}F-FDG uptake of Schmorl's node was located on the inferior borderline area surrounding the nucleus pulposus (thin arrow in C).

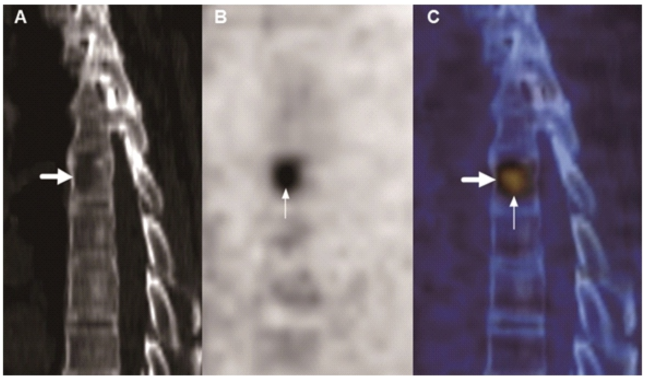

Figure 2. A 55 years old female with the history of breast cancer was diagnosed with vertebral metastases based on ^{18}F-FDG PET/CT. The SUVmax of the Schmorl's nodes was 5.4. The size of vertebral metastases on PET (thin arrow in B) was similar with that on CT (thick arrow in A). The image of PET almost overlapped to that of CT (thin and thick arrows in C).

jacent vertebra [10]. A number of theories have tried to explain the pathogenesis of Schmorl's nodes. Schmorl's nodes were considered a developmental disease [10], a degenerative bone disease [11], discs and vertebral bodies weakening disease [10], or an autoimmune disease [12]. Zhang et al. (2010) reported that the immune system played a key role in the development of symptomatic Schmorl's node because when a disc herniates into the vertebral endplate it could be considered as "non-self" tissue and in contact with blood would incite an immune reaction, edema, an influx of cytokines, and pain to the herniated material [12]. Other researchers also reported that the immune system played a role in symptomatic Schmorl's node formation as demonstrated by magnetic resonance imaging (MRI). Histologic examination of bone marrow from Schmorl's nodes patients showed evidence of inflammatory cell infiltration and bone marrow edema in the vicinity of the Schmorl's node [13]. Takahashi et al. (1995) reported that symptomatic Schmorl's node were seen as low-intensity lesions on T1-weighted MRI, but high-intensity on T2-weighted images, which were caused by the presence of inflammation [13]. This phenomenon can explain the high ^{18}F-FDG uptake in the bordeline area surrounding the pulpous nuclear that was higher than in other areas of Schmorl's nodes. Moreover, the high ^{18}F-FDG uptake of Schmorl's nodes was located in the borderline area surrounding the nucleus pulposus. Increased uptake and retention of ^{18}F-FDG has been shown in high concentration of inflammatory cells lesions [14]. Any inflammatory process can demonstrate hypermetabolic activity on ^{18}F-FDG PET/CT studies because of the high degree of glucose metabolism by inflammatory cells due to expression of high-concentration glucose transporters.

Bone metastases frequently happen in cancer patients. About 70% of patients with prostate cancer or breast cancer, and 15% to 30% of patients with colon, lung, bladder or renal cancer develop bone metastases [15]. Tumor cell dissemination to the bone is a complex process that involves reciprocal interplay between cancer cells, cells in the surrounding microenvironment, and the stroma itself [16]. Radiographic detection of bone metastases is most commonly performed by identifying sites of active bone remodeling [17]. Totally, the bone lesions arise as a function of the cancer/stroma interaction rather than as the detection of the cancer cells themselves. Bone metastases can be divided into osteolytic, osteoblastic, and/or of a mixed type. The destruction of bone by cancer cells is caused by the increasing number of osteoclasts rather than by the tumor cells [18]. In most bone destroying metastases, there is also an increase in new bone formation. Therefore, X-rays show a ring of new bone surrounding the destroyed bone [15]. In osteoblastic metastases, new bone formation is the primary feature. There-fore, the size of vertebral metastases on PET is larger or similar with that on CT. The images of PET almost overlapped completely that of CT in vertebral metastases lesion. It is well known that the ^{18}F-FDG PET has a higher sensitivity in the detection of osteolytic bone metastases and lower sensitivity in osteoblastic bone metastases compared with bone scan [19]. Recently, Uchida K et al. (2013) reported that PET in PET/CT could be a substitute for bone scan regarding the evaluation of spinal metastases, especially for patients with spinal osteolytic lesions identified by CT. With the increased application of whole-body ^{18}F-FDG PET/CT for the staging and follow-up of malignant disease, it is our opinion that ^{18}F-FDG PET/CT may support the diagnosis of Schmorl's nodes as related to vertebral metastases.

We recognized several limitations of this study. Firstly, this was a retrospective study with a small number of patients. Secondly, bone metastases included the osteolytic, osteoblastic, or mixed lesions. We know that ^{18}F-FDG PET/CT is more sensitive in detecting osteolytic or mixed lesions than the osteoblastic lesions [20]. Lytic lesions induce continuous bone removal and increased activity of tumor cells invasion with lysosomal enzymes, which act as osteoclastic process. In contrast, sclerotic lesions like fibrosis or collagen depositions do not contain many cells which can take up ^{18}F-FDG. Thirdly, some bone metastases were diagnosed by follow-up, not by pathology, which may influence the results. At the same time, we did not study the related findings in old or recent disc prolapse. Multicenter prospective studies with a larger number of patients are needed to confirm the result of the present study.

In conclusion, although the SUVmax in the Schmorl's nodes and in vertebral metastases was similar, the ^{18}F-FDG distribution characteristic in PET/CT can help differentiate the vertebral metastases from Schmorl's nodes.

Acknowledgment

Jigang YANG was supported by 2014 Beijing Excellent Talent Fund (No:2014000021223ZK45), Beijing Natural Science Foundation (No: 7152041).

The authors declare that they have no conflicts of interest

Bibliography

1. Mattei TA, Rehman AA. Schmorl's nodes: current pathophysiological, diagnostic, and therapeutic paradigms. *Neurosurg Rev* 2014; 37: 39-46.
2. Jin H, Yuan L, Li C et al. Diagnostic performance of FDG PET or PET/CT in prosthetic infection after arthroplasty: a meta-analysis. *Q J Nucl Med Mol Imaging* 2014; 58: 85-93.
3. Lin CY, Chen HY, Ding HJ et al. Evaluation of Schmorl's nodes using F-18 FDG PET/CT. *Clin Radiol* 2012; 67: e17-21.
4. Yang J, Zhen L, Zhuang H. Bone marrow metastases from alveolar rhabdomyosarcoma with impressive FDG PET/CT finding but less-revealing bone scintigraphy. *Clin Nucl Med* 2013; 38: 988-91.
5. Yang J, Codreanu I, Servaes S et al. Earlier detection of bone metastases from pleomorphic liposarcoma in a pediatric patient by FDG PET/CT than planar ^{99m}Tc MDP bone scan. *Clin Nucl Med* 2012; 37:e 104-7.
6. Niikura N, Hashimoto J, Kazama T et al. Diagnostic performance of F-fluorodeoxyglucose PET/CT and bone scintigraphy in breast cancer patients with suspected bone metastasis. *Breast Cancer* 2016; 23: 662-7
7. Zheng S, Dong Y, Miao Y et al. Differentiation of osteolytic metastases and Schmorl's nodes in cancer patients using dual-energy CT: advantage of spectral CT imaging. *Eur J Radiol* 2014; 83: 1216-21.
8. Park P, Tran NK, Gala VC et al. The radiographic evolution of a Schmorl's node. *Br J Neurosurg* 2007; 21: 224-7.
9. Chen YK, Chen HY, Kao CH. Schmorl's node may cause an increased FDG activity. *Clin Nucl Med* 2011; 36: 494-5.
10. Kyere KA, Than KD, Wang AC et al. Schmorl's nodes. *Eur Spine J* 2012; 21: 2115-21.
11. Hilton RC, Ball J, Benn RT. Vertebral end-plate lesions (Schmorl's nodes) in the dorsolumbar spine. *Ann Rheum Dis* 1976; 35: 127-32.
12. Zhang N, Li FC, Huang YJ et al. Possible key role of immune system in Schmorl's nodes. *Med Hypotheses* 2010; 74: 552-4.
13. Takahashi K, Miyazaki T, Ohnari H et al. Schmorl's nodes and low-back pain. Analysis of magnetic resonance imaging findings in symptomatic and asymptomatic individuals. *Eur Spine J* 1995; 4: 56-9.
14. Kubota R, Yamada S, Kubota K et al. Intratumoral distribution of fluorine-18-fluorodeoxyglucose in vivo: high accumulation in macrophages and granulation tissues studied by microautoradiography. *J Nucl Med* 1992; 33: 1972-80.
15. Roodman GD. Mechanisms of bone metastasis. *Discov Med* 2004; 4: 144-8.
16. Nguyen DX, Bos PD, Massague J. Metastasis: from dissemination to organ-specific colonization. *Nat Rev Cancer* 2009; 9: 274-84.
17. Ulmert D, Solnes L, Thorek D. Contemporary approaches for imaging skeletal metastasis. *Bone Res* 2015; 3: 15024.
18. Roodman GD. Biology of osteoclast activation in cancer. *J Clin Oncol* 2001; 19: 3562-71.
19. Uchida K, Nakajima H, Miyazaki T et al. ^{18}F-FDG PET/CT for Diagnosis of Osteosclerotic and Osteolytic Vertebral Metastatic Lesions: Comparison with Bone Scintigraphy. *Asian Spine J* 2013; 7: 96-103.
20. Liu NB, Zhu L, Li MH, et al. Diagnostic value of ^{18}F-FDG PET/CT in comparison to bone scintigraphy, CT and ^{18}F-FDG PET for the detection of bone metastasis. Asian Pacific journal of cancer prevention : *APJCP* 2013; 14: 3647-52.